Analyst

ROYAL SOCIETY OF CHEMISTRY

PAPER

View Article Online
View Journal | View Issue

Cite this: *Analyst*, 2023, **148**, 5525

Influence of bovine and human serum albumin on the binding kinetics of biomolecular interactions†

Benjamin Charron, Alexandre Delorme, Caroline Dubois, Maryam Hojjat Jodaylami and Jean-Francois Masson *

Bovine serum albumin (BSA) containing buffers are the standard blocking buffer in biosensing, yet human serum is the intended application for most clinical sensors. However, the effect of human serum albumin (HSA) on binding assays remains underexplored. A simple and well-studied assay (human IgG/goat anti-human IgG) was investigated with a surface plasmon resonance (SPR) sensor to address this fundamental question in sensing. Calibrations were performed with buffers containing various concentrations of bovine or human serum albumin, as well as full and diluted bovine or IgG-depleted human serum. It was found that HSA or human serum, but not BSA or bovine serum, significantly affected the SPR shift and binding constants of the assay. Interestingly, large differences were also observed depending on whether the animal or human antibody was immobilized on the SPR chip for detection , highlighting that matrix protein/analyte/receptor interactions play a significant role in the response. We find that the interaction of soluble HSA with human IgG interferes with the recognition region, affecting the binding constant, and thus results obtained in BSA are not necessarily applicable to clinical samples or *in vivo* conditions. We also clearly demonstrate why a minimum dilution of 1 : 10 is often required in SPR assays to remove most background effects. Taken together, these results show that: (1) BSA does not affect the binding constant between antibodies and thus serves its purpose well when only surface blocking is intended, (2) HSA is an adequate surrogate for human serum in assay optimization, and (3) blocking buffers should be prepared with HSA in the optimization steps of assays to be translated to human blood or serum.

Received 3rd July 2023,
Accepted 1st September 2023

DOI: 10.1039/d3an01117h

rsc.li/analyst

Introduction

The recent pandemic has further emphasized the importance of mobilizing the scientific community and healthcare services to develop a series of tools to characterize, identify, and treat an emerging disease. Among them, the rapid development of analytical tests or sensors, therapies, and vaccines are essential in controlling the spread of a virus.[1,2] On the longer term, serological tests[3–5] or sensors[6,7] that target antibodies in human serum or blood are needed to assess humoral immunity at the population level. To achieve that, sensors for antibodies need to work in biofluids, but the translation of sensors from the laboratory to clinical applications remains a bottleneck. Further understanding how biofluids interacts with the components of sensors and its impact on immunoassays is thus important, as well as finding good surrogate biological media for assay development.

Antibodies are large proteins produced by blood cells as one of the tools to protect the organism against viruses. They are composed of a constant domain (Fc) and two variable domains (Fab) that are highly specific to an antigen. The Fab domain is often used in sensors because of its high selectivity. This is one of the most common receptors used in sensors, but several problems can arise during an antibody assay. Other proteins or molecules may bind to the antibody in a non-specific manner.[8,9] Antibodies will have an affinity for a specific part of the analyte; in the case of a virus, usually a surface protein that must be immobilized on the surface of the sensor. Therefore, selecting the appropriate molecular receptor and placing it in the appropriate orientation to bind the antibody is critical to an efficient assay. However, this is only part of the problem, as the consideration of the matrix effect is key to developing sensors for clinical applications.[10] Antibodies circulate in blood, so an assay must be able to capture antibodies in a complex matrix either directly in blood or in (hopefully undiluted or moderately diluted) serum. In both cases,

Département de chimie, Quebec center for advanced materials (QCAM), Regroupement québécois sur les matériaux de pointe (RQMP), and Centre interdisciplinaire de recherche sur le cerveau et l'apprentissage (CIRCA), Université de Montréal, CP. 6128 Succ. Centre-Ville, Montréal, Qc, H3C 3J7, Canada. E-mail: jf.masson@umontreal.ca; Tel: +1-514-343-7342

† Electronic supplementary information (ESI) available. See DOI: https://doi.org/10.1039/d3an01117h

multiple background proteins can bind nonspecifically to the sensor or the surface-bound capture antigen[11] and affect sensor performance.

The development of protein-based sensors faces many challenges, such as the availability and high cost of capture proteins and the unavailability of human antibody standards. While these challenges are certainly important, we see another important challenge. Certified antibody-free serum is extremely rare and expensive, especially for COVID as the population is increasingly infected or vaccinated. This raises the simple but fundamental question of what is the most appropriate medium for optimizing assays and its impact on sensor performance for antibody detection.

Clinical samples are usually in the form of serum or whole blood, but in many cases the development of a serological sensor begins in buffer, a controlled environment simpler than blood. The most commonly used buffer is phosphate buffered saline (PBS) supplemented with bovine serum albumin (BSA). BSA is generally used to block potential nonspecific adsorption sites.[12] Serum albumin is the most common matrix protein and it is found at high concentrations of 3.5% to 5% in blood. Although BSA is used for other purposes, a protein of such importance in blood could provide insight into the effects of the blood or serum matrix would have on a sensor and the effects of human serum albumin (HSA) on biological assays are often overlooked. Proteins in solution can affect the assay in a number of ways, including by competing for the active site or by interfering with the mass transport of the components. Understanding how HSA affects the binding kinetics and how these results compare when translated to real matrices could greatly accelerate the development of future serological tests.

Here, we investigate the effect of the matrix composition on the kinetic and thermodynamic constants of a well-known antibody pair, human immunoglobulin G (IgG) and goat anti-human IgG. This interaction is studied in the presence of HSA to evaluate the effect of background proteins on a sensor in the context of clinical sensing. BSA is also studied as well to evaluate whether it could be used as a cheap yet effective buffer in preliminary tests towards clinical sensing. The sensor was developed based on a portable surface plasmon resonance (SPR) platform,[13,14] although we expect the results to be generally applicable to other SPR sensors or other sensing platforms. The suitability of SPR sensors for label-free and rapid clinical sensing has been demonstrated[15] for a wide range of biological targets including proteins and antibodies[16] and the results will then be extrapolated to bovine and human serum, which are more realistic matrices in the context of clinical sensing.

Experimental section

Materials

N-(3-Dimethylaminopropyl)-*N*′-ethylcarbodiimide hydrochloride (EDC, crystalline) and *N*-hydroxysuccinimide (NHS, 98%), bovine serum, bovine serum albumin (BSA, lyophilized powder, crystallized ≥98.0% (GE)), Human serum albumin (HSA, lyophilized powder, ≥96% (agarose gel electrophoresis)), were purchased from Sigma-Aldrich. Human Gamma Globulin (purified from non-immunized animal serum, IgG), goat anti-human IgG (H + L, polyclonal, Jackson Immunoresearch Labs), and human immunoglobulins (IgG, IgA, IgM, and IgE) depleted serum solution (Celprogen) were purchased from Cedarlane. Ferritin protein (from human liver) and rabbit anti-human ferritine (polyclonal) were purchased from MyBiosource. Recombinant Protein G was purchased from ThermoFisher. The anti-fouling peptide (3-mercaptopropionyl-LHDLHD, 98.35%) was obtained from Affinité Instruments.

Buffer preparation

The various running buffer solutions used in the experiments were diluted with PBS 1× (Fisher scientific) supplemented with 0.005% Tween (wt/vol, M.P. Biomedicals), when applicable, to keep the final Tween concentration constant at 0.005%. Stock solutions were prepared by dissolving either BSA or HSA at a concentration of 5% (m V^{-1}). Running buffer solutions with lower BSA or HSA concentrations (2.5%, 1%, 0.5%, 0.25%, and 0.1%) were prepared by diluting the corresponding 5% stock with PBS supplemented with 0.005% Tween. Bovine and human serum were fortified with 0.005% Tween, and serum was diluted (50% to 0.8% v/v) with PBS 1× supplemented with 0.005% Tween. These buffers were stored at 4 °C until use.

SPR experiments

Prior to the experiments, approximately 100 μL of the anti-fouling peptide solution (100 μM in dimethylformamide) was deposited on each prism and covered overnight to form a peptide monolayer with a free carboxyl terminus. The coated prisms were washed several times with anhydrous ethanol and deionized (DI) water to remove excess peptides, dried with nitrogen gas, and stored at 4 °C away from light. Each SPR experiment was performed on a P4SPR (Affinité instruments) using a freshly prepared SPR chip (Affinité Instruments). Surface functionalization with capture protein (human IgGs or goat anti-human IgGs) was performed using EDC–NHS cross-linking chemistry. Equal volumes of EDC (400 mM in DI water) and NHS (100 mM in DI water) solutions were thoroughly mixed for less than one minute and immediately injected onto the SPR chip. Activation of the peptide monolayer with the EDC–NHS solution was performed for 2 minutes before the solution was washed away with a 10 mM sodium acetate buffer at pH 4.5 prior to injection of the capture protein (20 μg mL^{-1} in 10 mM sodium acetate buffer, pH 4.5,[17,18] Fisher scientific). The capture protein solution was left in the cell for 20 minutes to bind the carboxyl surface *via* its primary amino group and then washed out with the 10 mM sodium acetate buffer at pH 4.5. The assay was continued from this step only if a binding shift of 2000 resonance units (RU), ±10%, was achieved. This corresponds to a binding shift of approximately 5.63 nm. Unreacted active sites were then blocked by injecting 1 M ethanolamine hydrochloride (in DI

water, adjusted to pH 8.5, Sigma-Aldrich) for 10 minutes. Finally, the running buffer for the experiment was injected and the signal allowed to stabilize before the next solution was injected. In experiments using protein G, protein G (20 μg mL^{-1} in 10 mM sodium acetate buffer pH 4.5) was injected after the EDC–NHS solution. Protein G was washed with sodium acetate buffer (10 mM pH 4.5) and unreacted sites were reacted with 1 M ethanolamine hydrochloride pH 8.5. The capture antibody was injected after washing away any remaining ethanolamine with the sodium acetate solution. The running buffer was then injected and stabilized prior to analyte injections.

Calibration curves in serum or buffer were then performed by injecting each analyte concentration (1, 2, 5, 10, 25, and 50 μg mL^{-1}) only after the previous binding curve had sufficiently stabilized, defined as an increase of less than 15% of the total curve shift in the last 10 minutes. Each injection of analyte was performed in triplicate in the analytical channels, while buffer was injected in the reference channel. Between each experiment with the instrument and before adding a new SPR chip, the tubing and fluidic cell were washed with 1 mL of a 10 mM glycine solution in DI water at pH 2.2 and 4 mL of DI water. The DI water was left in the cell and tubing overnight and washed with fresh DI water the next morning before drying the cell and changing the prism for the next experiment. It was noted that without this overnight cleaning procedure, a non-specific signal could sometimes be observed after water injection prior to surface functionalization.

Assays with ferritin and anti-ferritin as analyte and molecular receptor were performed in the same manner except that the sodium acetate solution was at pH 5.5, the anti-ferritin concentration used for surface functionalization was 10 μg mL^{-1}, and the injected analyte concentrations were 25, 50, 100, 200, 500, 1000 ng mL^{-1}.

Data processing

The acquired data were processed using TraceDrawer (RidgeView Instruments AB). The SPR sensorgrams were trimmed of the surface functionalization steps and injection spikes. The signal from the reference channel was then subtracted from the analysis signals, and injection spikes were deleted when necessary. Calculated SPR shifts were between the end of a concentration's binding curve and the baseline prior to each analyte injection. Kinetic evaluation was performed on each channel individually, without further processing, using a one-to-one model with depletion correction due to the absence of pumping in the experiment. The TraceDrawer evaluation directly provided the apparent kinetic constants of the antibody pair in the experimental condition.

Results and discussion

Calibration in PBS buffers supplemented with BSA or HSA

Protein–protein interaction is one of the hallmark experiments in SPR sensing. As such, a calibration curve was first established using a human IgG functionalized surface, where the binding partner was goat anti-human IgG in a buffer solution containing 0.1% of either HSA or BSA. Standard sensorgrams were obtained with both proteins and the expected Langmuir isotherm where SPR shifts reached a plateau at high analyte concentration was observed (Fig. 1 and S1†). This result shows that the experiment was well controlled, and that the proteins and molecules involved in the surface functionalization and analyte binding interacted as expected. The binding parameters offers a quantitative measure of the impact of BSA and HSA on the biomolecular interactions. In absence of impact of these proteins on the biomolecular interactions, the binding parameters should remains statistically invariable, as shown for buffers with 0.1% BSA or 0.1% HSA. The association rate constant (k_{on}) was 0.8×10^4 M^{-1} s^{-1} in BSA and 1×10^4 M^{-1} s^{-1} in HSA ($p = 0.19$), the dissociation rate constant (k_{off}) was 2×10^{-4} s^{-1} in both BSA and HSA ($p > 0.99$), and the dissociation constant (K_D) was 25 and 39 nM for BSA and HSA respectively ($p > 0.11$). Taken together, these results demonstrate statistical equivalency of HSA and BSA at a concentration of 0.1%.

The experiment was then reproduced with buffers containing higher fractions of BSA or HSA (Tables S1 and S2†). Results demonstrated that k_{on}, k_{off} and K_D were unaffected by the BSA concentration, with a value centered around 0.9×10^4 M^{-1} s^{-1}

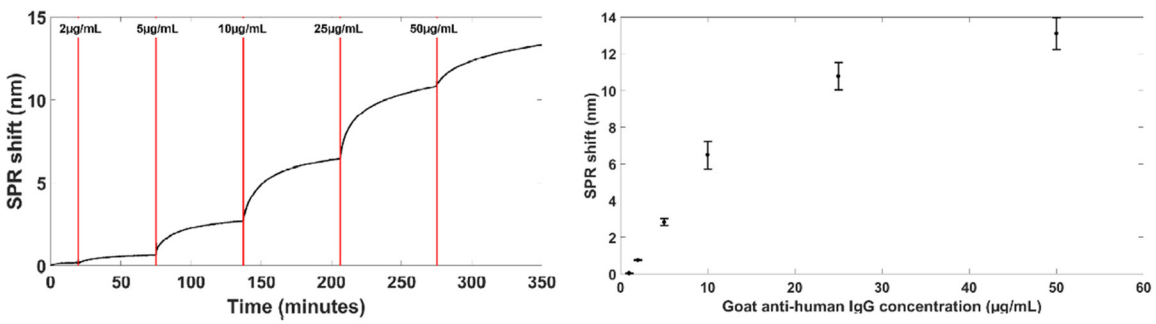

Fig. 1 Typical sensorgram for goat anti-human IgGs in 0.1% HSA running buffer on a human IgG functionalized surface (left) and corresponding Langmuir isotherm calibration curve (right). Red lines represent the injection of the next concentrations. Concentrations are 1, 2, 5, 10, 25, and 50 μg mL^{-1}.

for k_{on}, 2.5×10^{-4} s^{-1} for k_{off}, and 27 nM for K_D. This result could be expected since bovine proteins should not cross-react or interact with the goat and human proteins used in this binding assay. However, the kinetic and thermodynamic constants (Fig. 2 and 3) and the overall appearance of the sensorgrams (Fig. S2†) changed drastically as the HSA concentration was increased. Visually, as the HSA fraction increased, a higher analyte concentration was required to observe an SPR shift, meaning that null signals were observed at otherwise detectable concentrations in BSA (Fig. S2†). This was further exacerbated by the concentration of HSA in the running buffer, to the point that even the highest concentration (50 μg mL^{-1}) of goat anti-human IgG did not produce a signal at a 5% HSA fraction, making it impossible to calculate kinetic constants. It should be noted that the apparent unstabilized binding curves in Fig. S2† for the higher concentration are due to the scaling of the time axis. The signal from this injection alone was allowed to stabilize for over an hour, of which the last 10 minutes showed less than a 10% increase compared to the total shift. Also, the kinetic constant used here and throughout this study is the apparent constant of our goat polyclonal antibody and human gamma globulin. It is used as an average to compare the two buffer proteins and to describe the trends observed, not to define absolute values for the protein pair.

The presence of null signals for the lower concentrations also had a significant effect on the kinetic and thermodynamic constants calculations. k_{on} went from 1×10^4 M^{-1} s^{-1} to nearly zero as the HSA fraction increased from 0.1% to 0.5%. Even a concentration of 0.25% HSA was sufficient to reduce k_{on} by two orders of magnitude. This caused a significant increase in the time required to reach equilibrium for each concentration (Fig. S2†). Relatively speaking, k_{off} was moderately constant as it was equivalent to BSA at low HSA fractions, spiked moderately to 1.6×10^{-3} s^{-1} at 0.5% HSA and dropped back to near zero at 2.5% HSA, although the calculation at this concentration may be biased by the large proportion of null signals. K_D followed a similar trend to k_{off}, starting at 39 nM at 0.1% HSA and increasing to 0.5 mM at 0.5% HSA. Once again, the K_D calculation at 2.5% and 5% HSA was unreliable due to the large amount of null signals. The curves in HSA buffer, when converted to a concentration calibration plot, show variation in the sensitivity of the assay (Fig. 4). While some variation in the final binding shift can be observed due to varying amount of bound capture protein and measurement error, the general trend is that sensitivity is lower at high fractions of HSA.

These results may surprising at first, as they clearly show that small differences[19] between proteins of different mammalian origin in the buffer, especially at concentrations approach-

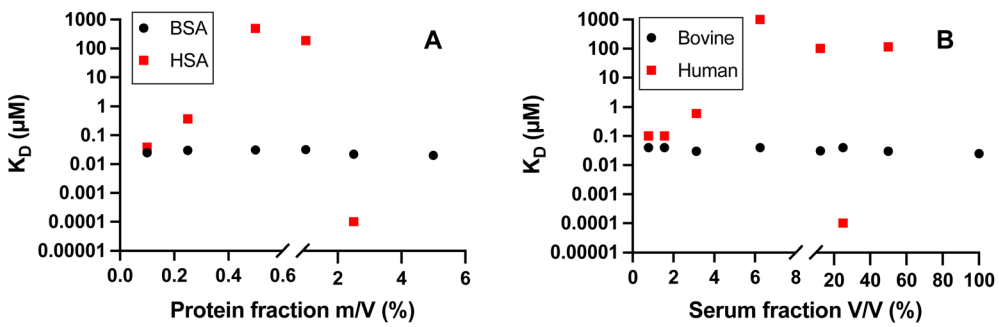

Fig. 2 (A) Influence of the protein content in the buffer on K_D with BSA (black) or HSA (red). (B) Influence of serum fraction (bovine (black) or human (red)) on K_D. Note that a protein fraction of about 5% in panel A corresponds to the same protein concentration as undiluted serum (100%, panel B).

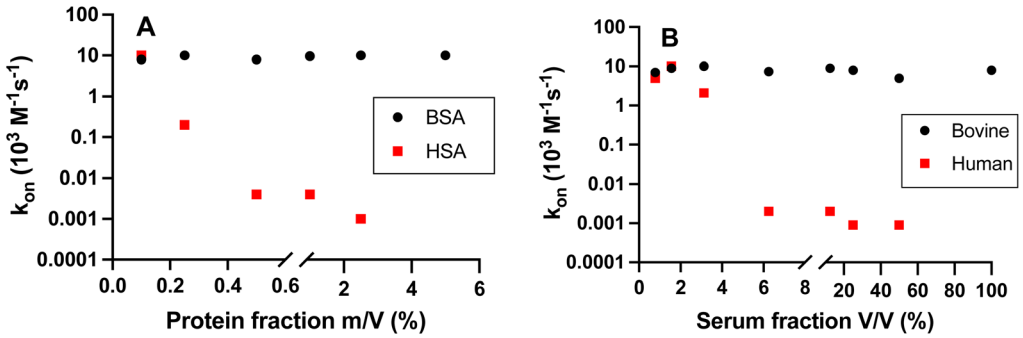

Fig. 3 (A) Influence of the protein content in the buffer on k_{on} with BSA (black) or HSA (red). (B) Influence of serum fraction (bovine (black) or human (red)) on k_{on}. Note that a protein fraction of about 5% in panel A corresponds to the same protein concentration as undiluted serum (100%, panel B).

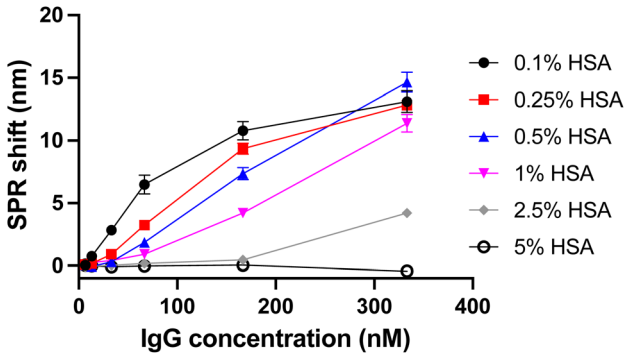

Fig. 4 Calibration plot for goat anti-human IgG in buffers with varying HSA concentration. Lines connecting data points guide the eye and do not represent a binding model.

ing that of biofluids, can have a drastic effect on the SPR assay. Importantly, the most significant effects were observed at HSA concentrations as low as 0.5%, corresponding to an approximate serum dilution of 1 : 10 (very common in clinical assays in SPR[15]). The decrease of k_{on} with HSA can be explained by the protein content of the buffer, which hinders the association of the analyte with the functionalized surface. In addition, HSA may hinder the mass transport of anti-IgG or occupy the binding sites on the human IgG surface, thus requiring a higher analyte concentration to displace the HSA. This may be supported by the fact that HSA is more hydrophobic than BSA.[20] HSA may therefore interact more with the antibodies, whether they are in solution or bound to the sensor's surface.

Another possible explanation could be due to different levels of fouling on the surfaces, altering the accessibility of surface-bound molecular receptors. A previous report showed no major differences in fouling between various sources of mammalian sera (bovine and chicken).[21] It is important to note that functionalization of low-fouling surfaces may alter the fouling performance and biorecognition activity.[22] As such, we verified that the differences in biomolecular interaction in the presence of the different matrices (BSA, HSA, bovine serum and human serum) were not related to different levels of surface fouling in the presence of these matrices. Each matrix was exposed to an SPR chip functionalized with human IgG and passivated with ethanolamine. Fouling was assessed as the shift of the baseline in running buffer measured before and after exposure of the surface to 1% BSA, 1% HSA, 1 : 5 dilution of bovine serum, and 1 : 5 dilution of Ig-depleted human serum. Bovine serum at 1 : 5 dilution had a significantly greater fouling at 1078 RU compared to 210 RU for Ig-depleted human serum at the same dilution, while 1% HSA or 1% BSA had 491 and 576 RU shifts, respectively. The difference in fouling from bovine and human serum can be explained by the absence of immunoglobulins in human serum, necessary given the nature of the immunoassay. Since bovine serum had the greatest fouling and no effect on the analytical response for the detection of anti-IgG, while human serum had the least fouling and the greatest effect on the analytical response, we conclude that fouling is not involved in reducing the response of the sensor in matrices with higher concentrations of background proteins in the matrix.

Effect of antibodies configuration and orientation

To further investigate the effect of the assay configuration on the human IgG and goat anti-human IgG pair, the previous calibration was repeated with the analyte and surface proteins exchanged. Thus, solutions of human IgGs were injected onto surface-bound goat anti-human IgGs. From these experiments, the influence of the buffer protein content on the mass transport of human IgG can be observed while the mass transport effect of goat anti-human IgG is eliminated.

Calibrations for the soluble human IgGs on a surface of goat anti-human IgGs were performed with buffers containing 0.1% or 5% HSA or BSA, respectively, covering the lower and upper limits investigated above. Experiments with 5% BSA or HSA did not result in significant plasmonic shifts. For some analyte injections, the signal even decreased slightly. This phenomenon could be due to the flow force displacing proteins that were weakly aggregated or nonspecifically adsorbed on the surface. Experiments with 0.1% BSA or HSA both showed a weak SPR shift at the lowest concentrations and did not increase further with injections of concentrations above 2 μg mL^{-1}, except for an increasing baseline (Fig. S4†). The observed shifts and the calculated maximum binding (B_{max}) for this assay were greatly reduced and consequently k_{on} is very high due to the rapid saturation of the surface (Table S3†). This result indicates that either both proteins effectively block binding sites in this assay configuration, or that a goat anti-human IgG surface provides fewer binding sites for human IgG than a human IgG surface under the same conditions. The lack of signal at higher albumin concentrations for both proteins indicates that some antibody binding is lost at high albumin concentrations, reducing the sensitivity of the assay.

We hypothesized that this last observation could be explained by improper orientation of the goat anti-human IgGs when using EDC–NHS coupling. Proper orientation of antibodies results in the Fab domain exposed to the solution, such that it remains available for binding the epitope it recognizes on human IgG. Failure to orient the antibodies with the Fab domain exposed to the solution leads to poor recognition of the target analyte and lower SPR response. The goat anti-human IgG is designed to capture the Fc domain of the human IgG *via* its Fab domains. Although EDC–NHS coupling is expected to bind the antibodies through the lysines that are mainly in the Fc region, a preferential Fab domain orientation on the surface could explain a loss of signal with the goat anti-human IgGs on the surface and a good signal with the human IgGs on the surface. When the goat anti-human IgGs are Fab-bound to the gold surface, capture of human IgGs becomes impossible, while the same configuration with the human IgGs exposes the Fc domain for capture of the goat anti-human IgG. The experiment was redesigned and protein G was used to bind the antibodies to the surface. Protein G binds the

Fc domains of antibodies from several species, including goat and human, and is commonly used to orient the Fc domain on the surface, exposing the Fab region.[23]

Fig. S5† shows the sensorgrams obtained when protein G was used to bind the capture antibody to the surface. With goat anti-human IgGs on the surface, the SPR shift at saturation increased from 1.5 to 3.4 nm with protein G. However, it remained significantly smaller than with human IgGs on the surface, where the SPR shift was 14.1 nm and increased to 17.6 nm after the 50 μg mL^{-1} analyte injection with protein G. Protein G resulted in a slightly higher calculated B_{max}, which resulted in a lower calculated k_{on} compared to the same assay configuration without protein G (Fig. 5 and Table S4†). Although protein G is assumed to be bound in a random orientation, this added layer of protein is favorable for antibody binding because it has 3 binding sites, potentially increasing the number of antibodies bound to the surface. As previously observed, when using a surface of goat anti-human IgG, the SPR shift saturated at lower analyte concentrations than with surface-bound human IgG, albeit at a concentration of 5 μg mL^{-1} with protein G as opposed to 2 μg mL^{-1} without protein G. In addition, as in experiments without protein G, the signal obtained with goat anti-human IgG on the surface was much smaller than that with human IgG. This affected the K_D measured with protein G (Fig. 5). Taken together, these results indicate that the decrease in signal is not due to improper orientation of the antibodies on the surface.

Calibrations in diluted serum

BSA and HSA are important and major components of bovine and human serum, respectively, but clinical analysis is faced with a more complex matrix. To evaluate how the previous results compare to the matrix for clinical samples, goat anti-human IgG calibrations on a human IgG surface were repeated with either bovine serum or IgG-depleted human serum. The experiment was performed with full serum and repeated by diluting the serum several times by 2 with the main buffer down to a 1 in 128 dilution. Kinetic and thermodynamic constants were obtained as before (Tables S5 and S6†).

The constants obtained with bovine serum were very stable over all of the serum dilutions and very similar to those obtained with BSA buffers (Fig. 2 and 3). With bovine serum k_{on}, k_{off}, and K_D averaged 8×10^3 M^{-1} s^{-1}, 2.9×10^{-4} s^{-1}, and 35 nM respectively, and were constant throughout the dilution series. As in previous experiments with BSA, all sensorgrams obtained with bovine serum showed the expected Langmuir isotherm, with the highest human IgG concentration (50 μg mL^{-1}) approaching surface saturation.

However, assays performed in IgG-depleted human serum showed no response at lower analyte concentrations when using undiluted or lightly diluted human serum. When full serum was used, no signal was obtained for any of the analyte concentrations (from 1 to 50 μg mL^{-1}). This effect diminished with more diluted serum, as the SPR sensor began to respond at lower analyte concentrations. This is consistent with the previous experiment using HSA, as serum dilution decreases the concentration of blood proteins, including human serum albumin.

This effect is clearly reflected in the K_D (Fig. 2) and k_{on} (Fig. 3) of this binding interaction in human serum. IgG-depleted human serum decreased k_{on} and increased K_D of the assay at low serum dilutions (1 : 16 dilution or less). Thus, it was not until the serum was diluted 32-fold that the binding constants were consistent with those expected in BSA or bovine serum. In particular, the calculated k_{on} constant increased with serum dilution, while k_{off} remained relatively stable (Table S6†). It is noteworthy that the IgG depleted serum contains less antibodies than the full unprocessed serum would have, as the IgG concentrations were at most 50 μg mL^{-1}, whereas the serum IgG concentration is usually in the mg mL^{-1} range. The current experiments were therefore performed in a somewhat simplified matrix and still had a drastic effect on the results. Nevertheless, these results in human serum are in good agreement with HSA, demonstrating that the use of a buffer containing the appropriate concentration of human serum albumin is a good approximation of how the serum would interact in a biological assay. Overall, these results demonstrate that bovine and human serum or

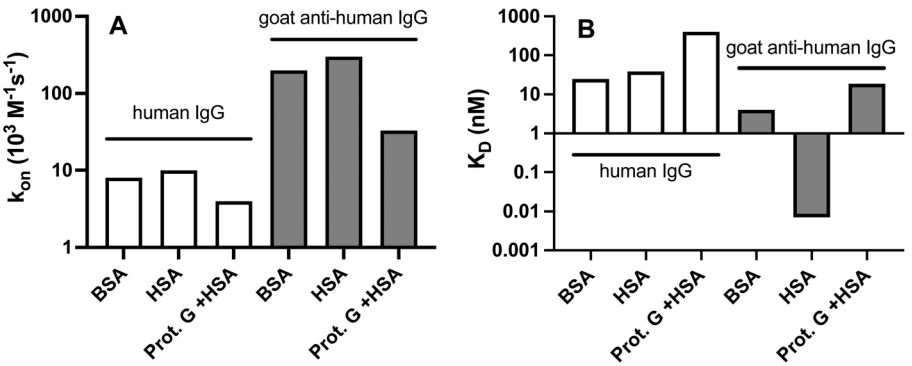

Fig. 5 Influence of the assay orientation and immobilization strategy on k_{on} (A) and K_D (B). Human IgG (white bars) or goat anti-human IgG (gray bars) were immobilized using EDC–NHS coupling or protein G (Prot.G), while the other protein was in solution. Assays were performed in 0.1% BSA or 0.1% HSA supplemented buffers.

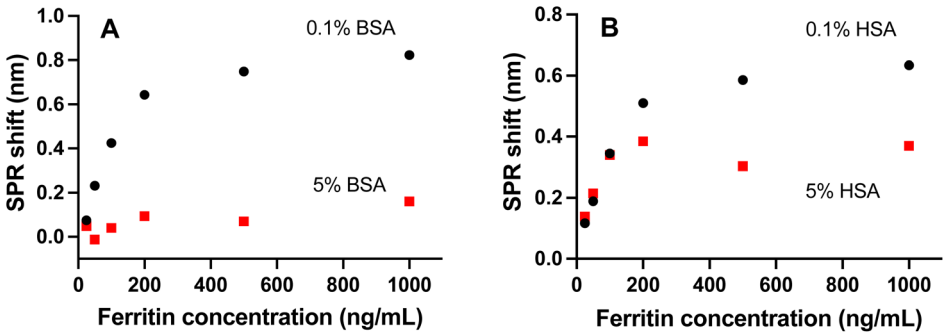

Fig. 6 Calibration curves for different BSA (A) and HSA (B) concentrations in running buffers.

albumin are not equivalent in biological assays. We believe this conclusion should be applicable to other biosensing platforms, especially for the ones using surface-bound molecular receptors, as the results show that the interaction between the binding partners are influenced by the molecular interaction of the background proteins with the analyte or receptor, and that this is not a result of the transduction mechanism.

Human ferritin and rabbit anti-ferritin

As a final validation step, the assay was performed with a different receptor/analyte pair. A surface functionalized with rabbit anti-human ferritin antibodies was used to capture human ferritin from the same BSA and HSA buffers as previously used for human IgG/anti-IgG. Anti-ferritin was immobilized at a pH of 5.5 and a concentration of 10 μg mL^{-1}, as this provided a better surface binding for this biomolecular interaction. Sodium acetate wash buffer was prepared at the same pH. The ferritin concentration in the buffer was also adjusted to match the range in which both minimal binding and saturation could be observed: concentrations between 25 and 1000 ng mL^{-1} were used. This assay was performed with both 0.1% and 5% concentrations of either BSA or HSA.

This protein pair showed much weaker binding and therefore very small wavelength shifts were obtained. As a result, the signal-to-noise level was lower and kinetic constants could not be extracted. Consequently, the results could only be analyzed qualitatively. Similar to the previous experiments, the measurements in a buffer with a low BSA and HSA concentration resulted in the expected Langmuir isotherm for both buffers (Fig. 6). There was a small difference between the buffers, as with 0.1% BSA in solution, a total SPR shift of 0.8 nm was obtained at surface saturation, while a buffer containing HSA resulted in a shift of 0.6 nm. This observation could be a result of the HSA interfering with the binding of the proteins.

In this case, higher BSA concentrations in the buffer did not lead to significant shifts, which can only be related to nonspecific binding, as no trend in ferritin concentration can be observed. During the assays, it was observed that the surface of the sensor was slightly disturbed by the injections, resulting in loss of signals, as if weakly bound proteins were washed away by the increased pressure, further supporting only nonspecific interactions. Similar to previous experiments with high HSA content, injection of ferritin solutions in 5% HSA running buffer resulted in lower SPR shifts, but the decrease in SPR shifts was less than for either the IgG sensor or the ferritin sensor in 5% BSA running buffer. Taken together, these results highlight the effect of high background protein concentrations on SPR sensors.

Conclusions

Several conclusions can be drawn from these results. BSA buffers provided controlled and repeatable binding assays with the expected Langmuir isotherm sensorgrams. The kinetic constants were stable and unaffected by changes in BSA concentration or the presence of bovine serum. Thus, BSA is an ideal background matrix for monitoring biomolecular interactions in a matrix that does not interfere with binding interactions. These experiments showed strong differences between bovine and human albumin or their sera, despite their structural similarities. A loss of antibody binding response was observed at higher concentrations of HSA in the buffer, which was more pronounced for IgG. It seems that HSA blocks the interaction between the binding partners or slows down the mass transport, since no effect was observed for k_{off}, but a marked decrease in k_{on} was observed for moderately diluted serum or high HSA concentrations. This effect could be due to the higher hydrophobicity of HSA compared to BSA, which may increase its interaction with the binding partners. We observed that these effects were minimized only at HSA dilutions greater than 10-fold, as 0.5% HSA still showed significant effects on the binding constants or on the SPR shifts. These observations were also made in IgG-depleted human serum, highlighting the similarities between HSA and human serum, making HSA a suitable surrogate for human serum in assay development. Calibration curves for ferritin showed similar SPR shifts for 0.1% BSA and HSA, but a large decrease in sensitivity for 5% BSA compared to a small decrease for 5% HSA. This observation shows that different proteins may interact differently with BSA and HSA, affecting sensor performance in matrices with high background protein. We conclude that

HSA should be used early in the development of buffers to accurately mimic the non-specific interactions and effects of human proteins on clinical assays. Otherwise, an assay optimized using bovine proteins or serum may prove difficult to translate to human clinical samples.

Conflicts of interest

JFM declares financial interest in Affinité Instruments.

Acknowledgements

We thank Joelle N. Pelletier and Adem H.-Parisien from Université de Montréal for their help and discussions. We acknowledge financial support from the Fonds de recherche du Québec – Nature et Technologies (FRQ-NT), the Natural Sciences and Engineering Research Council of Canada (NSERC), and the Canadian Foundation for Innovation (CFI).

References

1 Y. Liu, A. A. Gayle, A. Wilder-Smith and J. Rocklöv, The reproductive number of COVID-19 is higher compared to SARS coronavirus, *J. Travel Med.*, 2020, **27**(2), 1–4.

2 N. Ravi, D. L. Cortade, E. Ng and S. X. Wang, Diagnostics for SARS-CoV-2 detection: A comprehensive review of the FDA-EUA COVID-19 testing landscape, *Biosens. Bioelectron.*, 2020, **165**, 112454.

3 T. E. Miller, W. F. Garcia Beltran, A. Z. Bard, T. Gogakos, M. N. Anahtar, M. G. Astudillo, D. Yang, J. Thierauf, A. S. Fisch, G. K. Mahowald, M. J. Fitzpatrick, V. Nardi, J. Feldman, B. M. Hauser, T. M. Caradonna, H. D. Marble, L. L. Ritterhouse, S. E. Turbett, J. Batten, N. Z. Georgantas, G. Alter, A. G. Schmidt, J. B. Harris, J. A. Gelfand, M. C. Poznansky, B. E. Bernstein, D. N. Louis, A. Dighe, R. C. Charles, E. T. Ryan, J. A. Branda, V. M. Pierce, M. R. Murali, A. J. Iafrate, E. S. Rosenberg and J. K. Lennerz, Clinical sensitivity and interpretation of PCR and serological COVID-19 diagnostics for patients presenting to the hospital, *FASEB J.*, 2020, **34**(10), 13877–13884.

4 M. Infantino, M. Manfredi, V. Grossi, B. Lari, S. Fabbri, M. Benucci, A. Fortini, A. Damiani, E. M. Mobilia, M. Panciroli, S. Pancani and G. Pesce, Closing the serological gap in the diagnostic testing for COVID-19: The value of anti-SARS-CoV-2 IgA antibodies, *J. Med. Virol.*, 2021, **93**(3), 1436–1442.

5 A. Padoan, C. Cosma, L. Sciacovelli, D. Faggian and M. Plebani, Analytical performances of a chemiluminescence immunoassay for SARS-CoV-2 IgM/IgG and antibody kinetics %J Clinical Chemistry and Laboratory Medicine (CCLM), *Clin. Chem. Lab. Med.*, 2020, **58**(7), 1081–1088.

6 A. David, L. Scott, S. Jugwanth, M. Gededzha, T. Kahamba, N. Zwane, N. Mampeule, I. Sanne, W. Stevens and E. S. Mayne, Operational characteristics of 30 lateral flow immunoassays used to identify COVID-19 immune response, *J. Immunol. Methods*, 2021, **496**, 113096.

7 M. Krone, J. Gütling, J. Wagener, T.-T. Lâm, C. Schoen, U. Vogel, A. Stich, F. Wedekink, J. Wischhusen, T. Kerkau, N. Beyersdorf, S. Klingler, S. Backes, L. Dölken, G. Gasteiger, O. Kurzai, A. Schubert-Unkmeir and Y.-W. Tang, Performance of Three SARS-CoV-2 Immunoassays, Three Rapid Lateral Flow Tests, and a Novel Bead-Based Affinity Surrogate Test for the Detection of SARS-CoV-2 Antibodies in Human Serum, *J. Clin. Microbiol.*, 2021, **59**(8), e00319–e00321.

8 L. Rajaković, V. Ghaemmaghami and M. Thompson, Adsorption on film-free and antibody-coated piezoelectric sensors, *Anal. Chim. Acta*, 1989, **217**, 111–121.

9 A. Ahluwalia, G. Giusto and D. De Rossi, Non-specific adsorption on antibody surfaces for immunosensing, *Mater. Sci. Eng., C*, 1995, **3**(3), 267–271.

10 J.-F. Masson, Consideration of Sample Matrix Effects and "Biological" Noise in Optimizing the Limit of Detection of Biosensors, *ACS Sens.*, 2020, **5**(11), 3290–3292.

11 C. Blaszykowski, S. Sheikh and M. Thompson, Surface chemistry to minimize fouling from blood-based fluids, *Chem. Soc. Rev.*, 2012, **41**(17), 5599–5612.

12 R. S. Moura, G. O. Penna, T. Fujiwara, M. A. d. A. Pontes, R. Cruz, H. d. S. Gonçalves, M. L. F. Penna, L. P. V. Cardoso, M. M. d. A. Stefani and S. Bührer-Sékula, Evaluation of a rapid serological test for leprosy classification using human serum albumin as the antigen carrier, *J. Immunol. Methods*, 2014, **412**, 35–41.

13 J.-F. Masson, Portable and field-deployed surface plasmon resonance and plasmonic sensors, *Analyst*, 2020, **145**(11), 3776–3800.

14 S. S. Zhao, N. Bukar, J. L. Toulouse, D. Pelechacz, R. Robitaille, J. N. Pelletier and J.-F. Masson, Miniature multi-channel SPR instrument for methotrexate monitoring in clinical samples, *Biosens. Bioelectron.*, 2015, **64**, 664–670.

15 J.-F. Masson, Surface Plasmon Resonance Clinical Biosensors for Medical Diagnostics, *ACS Sens.*, 2017, **2**(1), 16–30.

16 J. Homola, Surface Plasmon Resonance Sensors for Detection of Chemical and Biological Species, *Chem. Rev.*, 2008, **108**(2), 462–493.

17 M. Hojjat Jodaylami, A. Djaïleb, P. Ricard, É. Lavallée, S. Cellier-Goetghebeur, M.-F. Parker, J. Coutu, M. Stuible, C. Gervais, Y. Durocher, F. Desautels, M.-P. Cayer, M. J. de Grandmont, S. Rochette, D. Brouard, S. Trottier, D. Boudreau, J. N. Pelletier and J.-F. Masson, Cross-reactivity of antibodies from non-hospitalized COVID-19 positive individuals against the native, B.1.351, B.1.617.2, and P.1 SARS-CoV-2 spike proteins, *Sci. Rep.*, 2021, **11**(1), 21601.

18 A. Djaileb, M. Hojjat Jodaylami, J. Coutu, P. Ricard, M. Lamarre, L. Rochet, S. Cellier-Goetghebeur, D. Macaulay, B. Charron, É. Lavallée, V. Thibault, K. Stevenson, S. Forest, L. S. Live, N. Abonnenc, A. Guedon, P. Quessy, J.-F. Lemay, O. Farnós, A. Kamen, M. Stuible, C. Gervais, Y. Durocher, F. Cholette, C. Mesa, J. Kim,

M.-P. Cayer, M.-J. de Grandmont, D. Brouard, S. Trottier, D. Boudreau, J. N. Pelletier and J.-F. Masson, Cross-validation of ELISA and a portable surface plasmon resonance instrument for IgG antibody serology with SARS-CoV-2 positive individuals, *Analyst*, 2021, **146**(15), 4905–4917.

19 K. A. Majorek, P. J. Porebski, A. Dayal, M. D. Zimmerman, K. Jablonska, A. J. Stewart, M. Chruszcz and W. Minor, Structural and immunologic characterization of bovine, horse, and rabbit serum albumins, *Mol. Immunol.*, 2012, **52**(3), 174–182.

20 R. Maier, M. R. Fries, C. Buchholz, F. Zhang and F. Schreiber, Human versus Bovine Serum Albumin: A Subtle Difference in Hydrophobicity Leads to Large Differences in Bulk and Interface Behavior, *Cryst. Growth Des.*, 2021, **21**(9), 5451–5459.

21 M. V. Riquelme, H. Zhao, V. Srinivasaraghavan, A. Pruden, P. Vikesland and M. Agah, Optimizing blocking of nonspecific bacterial attachment to impedimetric biosensors, *Sens Biosensing Res*, 2016, **8**, 47–54.

22 H. Vaisocherová, V. Ševců, P. Adam, B. Špačková, K. Hegnerová, A. de los Santos Pereira, C. Rodriguez-Emmenegger, T. Riedel, M. Houska, E. Brynda and J. Homola, Functionalized ultra-low fouling carboxy- and hydroxy-functional surface platforms: functionalization capacity, biorecognition capability and resistance to fouling from undiluted biological media, *Biosens. Bioelectron.*, 2014, **51**, 150–157.

23 L. Björck and G. Kronvall, Purification and some properties of streptococcal protein G, a novel IgG-binding reagent, *J. Immunol.*, 1984, **133**(2), 969–974.